JACS
JOURNAL OF THE AMERICAN CHEMICAL SOCIETY
Article
pubs.acs.org/JACS

1,3-Cationic Alkylidene Migration of Nonclassical Carbocation: A Density Functional Theory Study on Gold(I)-Catalyzed Cycloisomerization of 1,5-Enynes Containing Cyclopropene Moiety

Qinghai Zhou and Yuxue Li*

State Key Laboratory of Organometallic Chemistry, Shanghai Institute of Organic Chemistry, Chinese Academy of Sciences, 345 Lingling Road, Shanghai 200032, People's Republic of China

Supporting Information

ABSTRACT: For quite a long time, nonclassical carbocations have only been regarded as special intermediates with limited cases in solvolysis reactions. However, the present work shows that in common reaction, typical nonclassical carbocations may be involved in and have significant effects on the reaction mechanisms. In this work, DFT studies have been performed on the mechanism of gold(I)-catalyzed cycloisomerization of 1,5-enynes containing cyclopropene moiety at PBE1PBE/6-31+G**/SDD level. An unprecedented pathway containing two consecutive 1,3-cationic alkylidene migrations of nonclassical carbocation intermediates derived from norbornenyl cation, rather than the generally considered Wagner−Meerwein 1,2-alkyl migrations, was found. Detailed structural analysis shows the nature of this 1,3-cationic alkylidene migration: it is promoted by strong cation−π interaction between the cationic center and the double bond. Topological analysis shows that for certain nonclassical carbocation intermediates (**1c′-A** and **1c′-F**), there do exist bond critical point and bond path between the cationic center and the double bond. On the basis of the mechanisms proposed, the product selectivity controlled by the substituent effects was also rationalized.

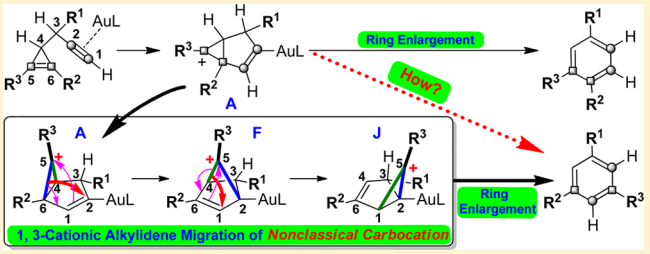

INTRODUCTION

In the past few years, gold catalysis[1] has been intensively studied for its advantages such as mild reaction conditions under room temperature, no need for inert atmosphere, and diverse reaction modes. Among gold-catalyzed reactions, cycloisomerization of enynes[2−5] has drawn much attention, as this type of reaction transforms linear, simple, and easy-to-get substrates into various useful synthons in synthetic chemistry with high yield and atom economy. Generally, the gold(I)-catalyzed cycloisomerization of normal 1,5-enynes gives [3.1.0] bicyclic compounds or cyclohexadiene compounds, and it is commonly accepted that the Wagner−Meerwein 1,2-alkyl migrations are often involved in the rearrangements of the carbocation skeleton.[2−4,6]

Recently, Wang and co-workers[7] connected C4 and C6 in the normal 1,5-enyne skeleton with a single bond (Scheme 1A), introducing cyclopropene moiety into the substrate. The typical reaction conditions and substrates are listed in Scheme 1B.[8] This gold(I)-catalyzed cycloisomerization of enyne **1** affords benzene derivatives rapidly in high yields at room temperature. The product distribution can be controlled by the substituents, involving cleavages of both the carbon−carbon triple (C1≡C2) and the double (C5═C6) bonds (product **3**) or neither of them (product **2**) to afford mixed products (for **1a**) or solo product (for **1b**−**1d**), respectively.

Mechanisms were proposed[7] as shown in Scheme 2. The initial cyclization affords the vinyl gold intermediate **A**.

Scheme 1. (A) Normal 1,5-Enyne and 1,5-Enyne Containing Cyclopropene Moiety; and (B) Typical Conditions and Substrates for the Gold(I)-Catalyzed Cycloisomerization of 1,5-Enynes Containing Cyclopropene Moiety

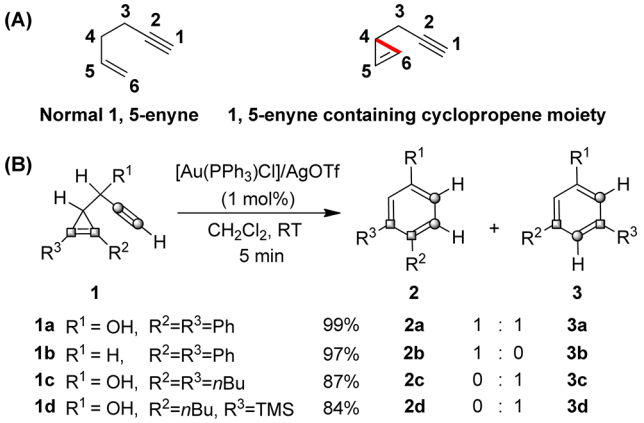

1a	R^1 = OH, R^2=R^3=Ph	99%	**2a**	1	: 1	**3a**
1b	R^1 = H, R^2=R^3=Ph	97%	**2b**	1	: 0	**3b**
1c	R^1 = OH, R^2=R^3=*n*Bu	87%	**2c**	0	: 1	**3c**
1d	R^1 = OH, R^2=*n*Bu, R^3=TMS	84%	**2d**	0	: 1	**3d**

Subsequently, the reaction diverges into ***Path-1*** and ***Path-2***. Along ***Path-1***, ring-enlargement of **A** and 1,2-H migration lead to product **2**. ***Path-2*** accounts for the formation of the double-cleavage product **3**. The back-donation of the gold atom in **A**

Received: October 21, 2013
Published: December 31, 2013

dx.doi.org/10.1021/ja410734e | *J. Am. Chem. Soc.* 2014, 136, 1505−1513

Scheme 2. Mechanisms Proposed for the Gold(I)-Catalyzed Cycloisomerization of 1,5-Enynes Containing Cyclopropene Moiety in Ref 7

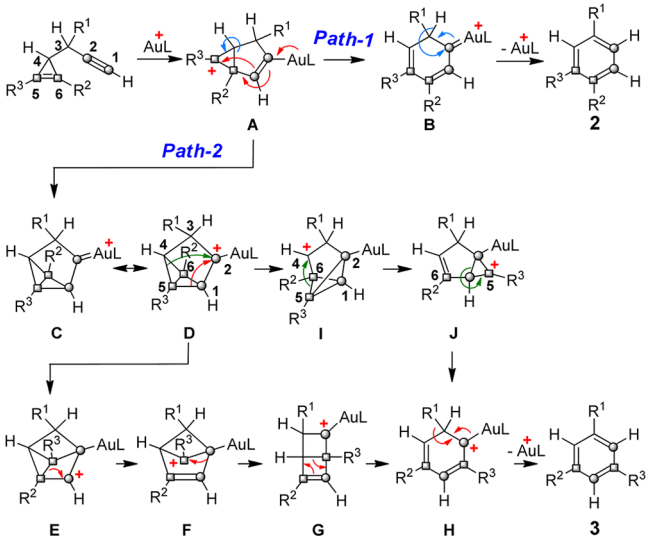

leads to **C** or **D**. 1,2-Alkyl migration of **D** then yields **E**, bond breaking of **E** generates **F**, and another 1,2-migration forms the Dewar benzene-type intermediate **G**. Ring-enlargement of **G** leads to **H**, and subsequent 1,2-H migration affords the final product **3**. Alternatively, **D** may transform to **I** via 1,3-alkyl migration, and subsequently yield **H**.

However, our test calculations show that the key intermediate **G** is not a stationary point on the potential energy surface, and **I** is not a minimum, but like a transition structure between **F** and **J**.[8] These results indicate that there must be new pathways between intermediate **A** and product **3**. Kozmin et al. suggested that the double-cleavage products of cycloisomerization of siloxy-substituted 1,5-enynes are generated via 1,2-alkyl migrations. This mechanism has been supported by DFT calculations.[3,4] The double-cleavage products of cycloisomerization of 1,6-enynes resulted from a concerted homoallylic cation rearrangement via a four-membered ring transition state, which has been well studied by Echavarren and Yu et al.[5] Although several theoretical studies[4] have been done on the cycloisomerization of normal 1,5-enynes, the mechanism of the present case to form the double-cleavage product is indeed intriguing.

In this Article, we proposed a mechanism characterized by two consecutive 1,3-cationic alkylidene migrations of typical nonclassical carbocation intermediates derived from norbornenyl cation. It is apparently different from the commonly called 1,3-carbon and 1,3-alkylidiene migration,[9a−c] because the migrated group here is a carbocation and the cationic center remains unchanged during the process. Nonclassical carbocations have been proposed to participate in the skeletal rearrangement in metal-catalyzed isomerization of enynes.[9g−j] However, detailed theoretical studies and clear structural analyses are seldom.[9j] Here, this idea was confirmed further by our study.

Since the discovery of norbornyl and norbornenyl cation by Winstein and Trifan in 1949 and 1955, so many famous groups have been dedicated to the study of nonclassical carbocations.[10−12] Schleyer, Olah, Houk, etc., did profound theoretical studies. After more than a half century, a breakthrough has been made recently by Krossing et al., when the crystallographic proof of nonclassical 2-norbornyl cation was obtained.[10o] However, for quite a long time, people used to think that nonclassical carbocations are only special intermediates with limited cases. The present work indicates that typical nonclassical carbocations possibly exist in common chemical reactions, acting as an important intermediate, and exerting significant effects on the reaction mechanisms.

MODELS AND METHODS

To disclose the reaction mechanisms, DFT[13] studies using the PBE1PBE[14] method with Gaussian 09[15] program have been performed. Recent test calculations show that PBE0 is one of the best functionals to calculate gold complexes.[16] For C, H, O, and P, the 6-31+G** basis set was used; and for the Au atom, the SDD basis set with effective core potential (ECP)[17] was used. Harmonic vibrational frequencies were calculated to identify all stationary points to be either minima (with zero imaginary frequencies) or transition states (with one imaginary frequency). Selected transition states have been checked by intrinsic reaction coordinate (IRC) calculations.[8] The Hirshfeld atomic charges were calculated by the Multiwfn program.[8,18] The solvent effect was estimated by the IEFPCM[19] method with UAHF radii in dichloromethane (ε = 8.93) using the Gaussian 03[20] program.

RESULTS AND DISCUSSION

Cyclization Pathways. First, substrate **1a** was used to explore the whole reaction pathways.[8] As shown in Scheme 3

Scheme 3. Calculated 5-*endo-dig* and 4-*exo-dig* Cyclization Pathways of the Reactant Complex 1a-R[a]

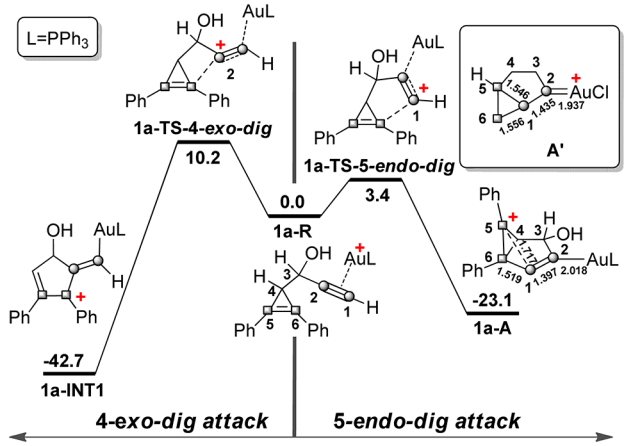

[a] **A'** is a cyclization intermediate of normal 1,5-enyne taken from ref 4c (reoptimized).[8] The relative free energies in dichloromethane (298.15 K, 1.0 atm) are in kcal/mol, calculated at the PBE1PBE/6-31+G**/SDD level.

and Figure 1, the gold catalyst coordinates with substrate **1a** forming the reactant complex **1a-R**. The π-electron of the double bond in the cyclopropene moiety then attacks the C≡C triple bond. The energy barrier of 4-*exo-dig* cyclization is much higher than that of 5-*endo-dig* cyclization (10.2 kcal/mol vs 3.4 kcal/mol). The 5-*endo-dig* cyclization transition state **1a-TS-5-*endo-dig*** contains a five-membered ring. The C2−C3−C4 angle is 105.8°, which is close to the ideal bond angle in an sp^3-hybridized carbon atom (109.5°), whereas in the 4-*exo-dig* cyclization transition state **1a-TS-4-*exo-dig***, there is a four-membered ring with a C2−C3−C4 angle of 94.9°. Obviously, the ring strain is a main factor controlling the selectivity in the cyclization step.

dx.doi.org/10.1021/ja410734e | J. Am. Chem. Soc. 2014, 136, 1505−1513

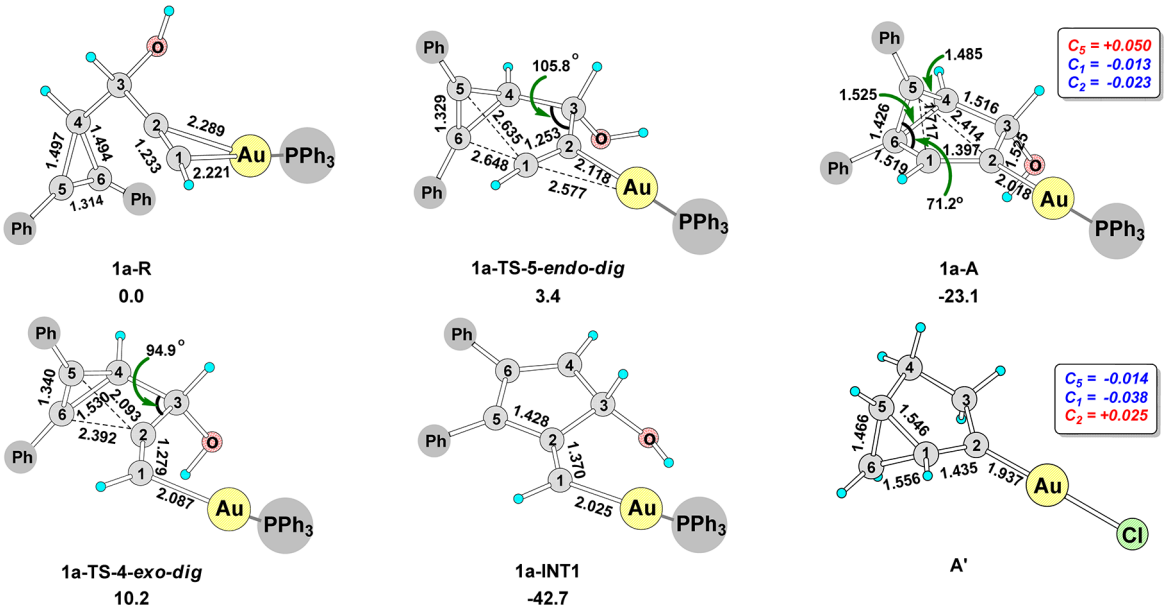

Figure 1. The optimized structures on the cyclization pathways with selected bond lengths (in Å), bond angles (in degrees), and Hirshfeld atomic charges (positive in red, negative in blue). The structure of **A**′ is also given. The relative free energies in solvent ΔG_{sol} (298.15 K, 1.0 atm) are in kcal/mol. The details of the Ph groups and the PPh_3 ligand are not shown for clarity. Calculated at the PBE1PBE/6-31+G**/SDD level.

Scheme 4. Calculated Direct Ring-Enlargement (*Path-1*) and 1,3-Cationic Alkylidene Migration (*Path-3*) Pathways of the Vinyl Gold Intermediate 1a-A[a]

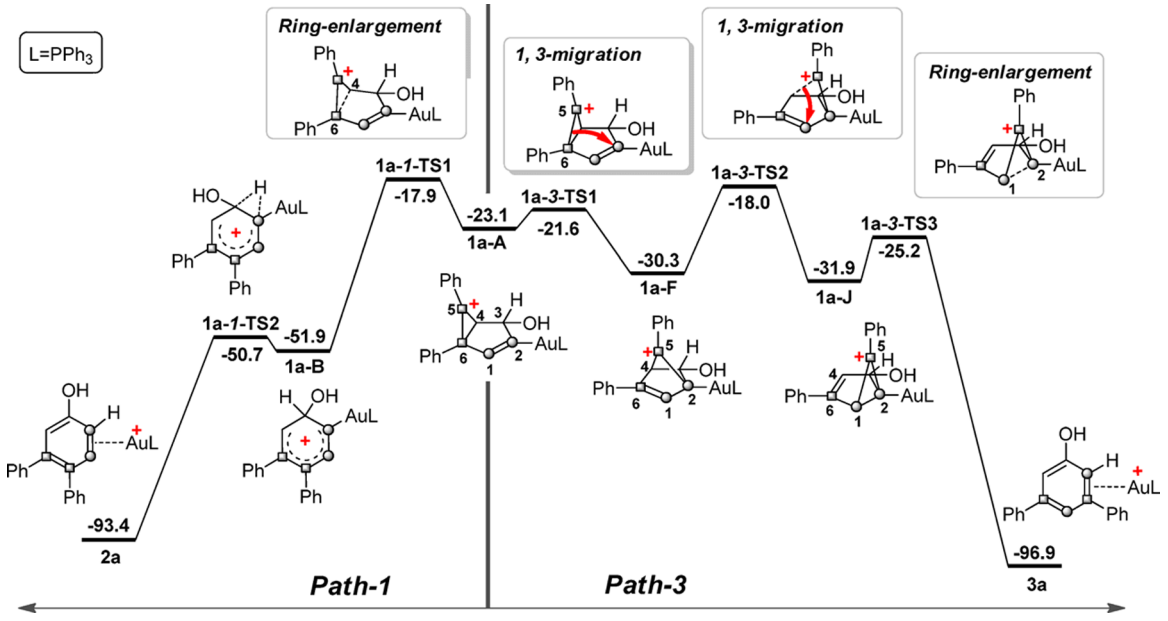

[a]The relative free energies in dichloromethane ΔG_{sol} (298.15 K, 1.0 atm) are in kcal/mol. Calculated at the PBE1PBE/6-31+G**/SDD level.

For normal 1,5-enynes,[4c] in the bicyclo intermediate **A**′ (Scheme 3 and Figure 1), C1 forms a full C−C bond with both C5 and C6 (1.546 and 1.556 Å), and the C1−C2 bond is elongated to 1.435 Å. The formal positive charge localizes on C2 and the Au atom, and may promote the subsequent 1,2-alkyl migrations. However, in **1a-A**, the C4−C6 bond prevents C1 and C5 from forming a full σ-bond, and the C1−C5 distance is much longer (1.717 Å). Thus the formal positive charge localizes on C5, and the C1−C2 bond largely remains a double bond (1.397 Å). These differences between **1a-A** and **A**′ lead to different pathways in the subsequent reactions.

Ring-Enlargement Pathway (*Path-1*). As shown in the left part of Scheme 4 and Figure 2, along ***Path-1***, the original C4−C6 bond breaks (**1a-1-TS1**), leading to intermediate **1a-B**. Subsequent 1,2-H migration (**1a-1-TS2**) affords the final product **2a**, accompanied by the regeneration of the gold catalyst. This pathway is similar to that of normal 1,5-enynes, which breaks the C1−C5 bond in the ring-enlargement process and leads to the cyclohexadiene products.[4c]

1,3-Cationic Alkylidene Migration Pathway (*Path-3*). In our test calculations, only the intermediates **A**, **F**, **J**, and **H** in ***Path-2*** (Scheme 2) were successfully located.[8] Inspired by these findings, we proposed a new reaction pathway to go

dx.doi.org/10.1021/ja410734e | J. Am. Chem. Soc. 2014, 136, 1505−1513

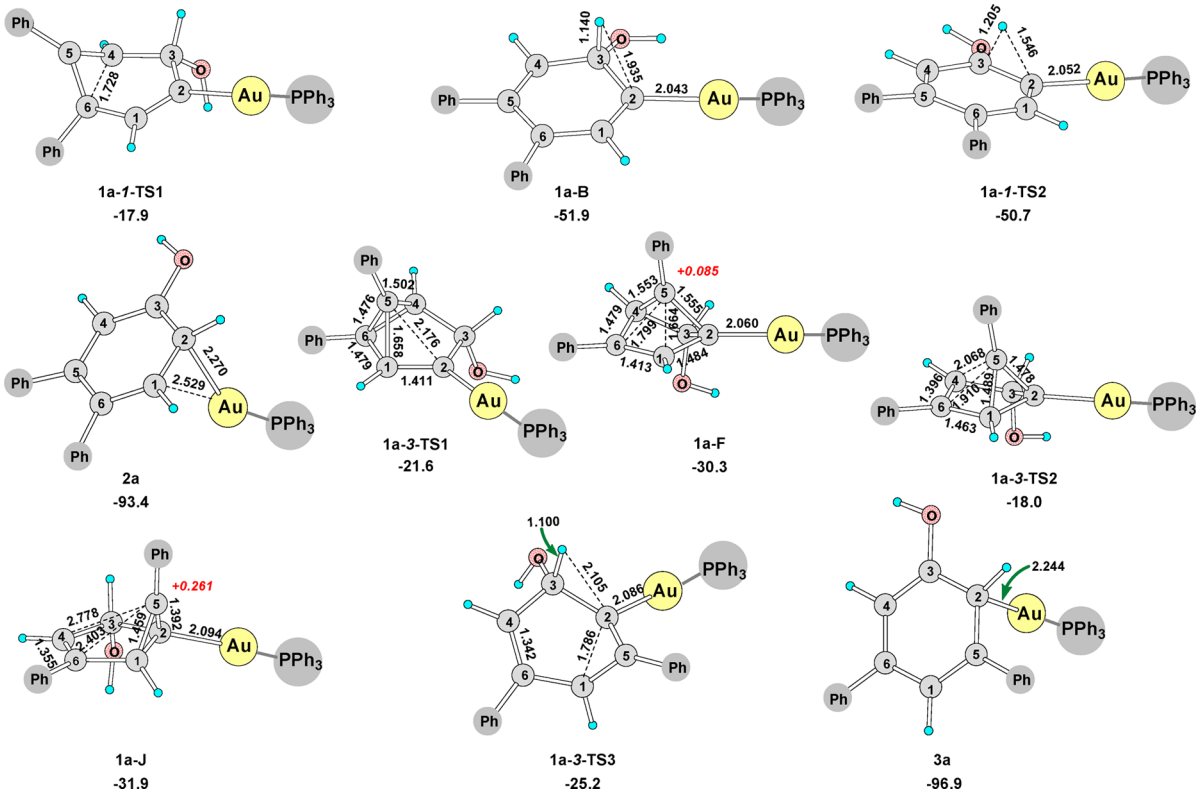

Figure 2. The optimized structures on ***Path-1*** and ***Path-3*** with selected bond lengths (in Å) and Hirshfeld atomic charges (in red). The relative free energies in solvent ΔG_{sol} (298.15 K, 1.0 atm) are in kcal/mol. Details of the Ph groups and the PPh_3 ligand are not shown for clarity. Calculated at the PBE1PBE/6-31+G**/SDD level.

through these possible intermediates. As shown in Scheme 5, the initial cyclization intermediate **A** undergoes 1,3-cationic alkylidene migration, breaking the C5−C6 bond and forming the C5−C2 bond to afford **F**, and another 1,3-cationic alkylidene migration breaking the C5−C4 bond and forming the C5−C1 bond leads to **J**. The following ring-enlargement of **J** breaks the C1−C2 bond, yielding the final double-cleavage product **3**. This process can be envisioned as a tertiary carbocation walking and turning around on a pentadiene framework.

Scheme 5. New Mechanism Proposed for the Cycloisomerization (*Path-3*)

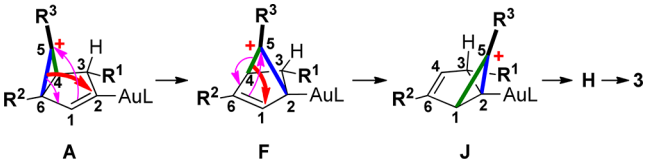

As shown in Scheme 4 and Figure 2, in the first 1,3-cationic alkylidene migration (**1a-3-TS1**), the π-electrons of the C1═C2 double bond in **1a-A** attack the cationic center C5. Over a small barrier of 1.5 kcal/mol, the C5−C2 bond forms, the C5−C6 bond breaks, and the C1−C2 double bond simultaneously migrates to C1−C6, leading to bicyclo[2.1.1]hexene intermediate **1a-F**. Thus the cationic center C5 migrates from C6 to the Au-linked carbon C2. The C5−C6 bond break corresponds to the C═C double bond break in substrate **1a**. Subsequently, **1a-F** undergoes a further 1,3-cationic alkylidene migration via transition state **1a-3-TS2** over a barrier of 12.3 kcal/mol. In this process, the π-electrons of **1a-F** on C1 attack C5, forming C5−C1 bond, and the C1−C6 double bond migrates to C6−C4, leading to intermediate **1a-J**. Next, the concerted[4c,8] ring-enlargement and 1,2 H-migration (**1a-3-TS3**) over a barrier of 6.7 kcal/mol leads to the double-cleavage product **3**, accompanied by the regeneration of the gold catalyst. It is interesting that both **1a-A** and **1a-J** have bicyclo[3.1.0]hexene backbones, and undergo a similar ring-enlargement process to form the final products. The largest barrier of this reaction is 12.3 kcal/mol, which is well consistent with the fact that the reaction is completed within 5 min.

Nonclassical Carbocation Intermediates in the Reaction. The intermediates **1a-A** and **1a-F** bring to mind the famous nonclassical 2-norbornenyl carbocation (Scheme 6A).[10−12] They have similar structures in which the cationic center is stabilized by π-donation of the neighboring double bond. Furthermore, **1a-F** is very similar to the bicyclo[2.1.1]-hex-2-en-5-ylium cation (**M**).[10k,l,11a] In the 2-norbornenyl cation, the distances between the cationic center and the carbon atoms of the double bond are 1.88 and 1.87 Å, respectively.[10j,l] In **M** these distances are 1.741 and 1.744 Å, respectively.[10k,l] In **1a-A**, the cationic center C5 faces the double bond unsymmetrically. Therefore, C5 has a stronger interaction with the alkene carbon C1 (C5−C1 = 1.717 Å) than with C2 (C5−C2 = 2.414 Å). **1a-F** has more symmetrical structure (C5−C6 = 1.799 Å, C5−C1 = 1.664 Å), and is 7.2 kcal/mol more stable than **1a-A**. In **1a-F**, a styrene fragment comes into being. The conjugation of the phenyl group with the double bond, and better electron donation to the cationic center C5 may account for its stability. However, in **1a-J**, C5−C4 and C5−C6 are 2.778 and 2.403 Å, respectively, indicating

dx.doi.org/10.1021/ja410734e | J. Am. Chem. Soc. 2014, 136, 1505−1513

Scheme 6. (A) Famous Nonclassical 2-Norbornenyl Cation, Bicyclo[2.1.1]hex-2-en-5-ylium Cation (M), and Intermediates 1a-A and 1a-F in the Isomerization Reaction; and (B) Classical Carbocation Resonance Structures of 1a-A and 1a-F

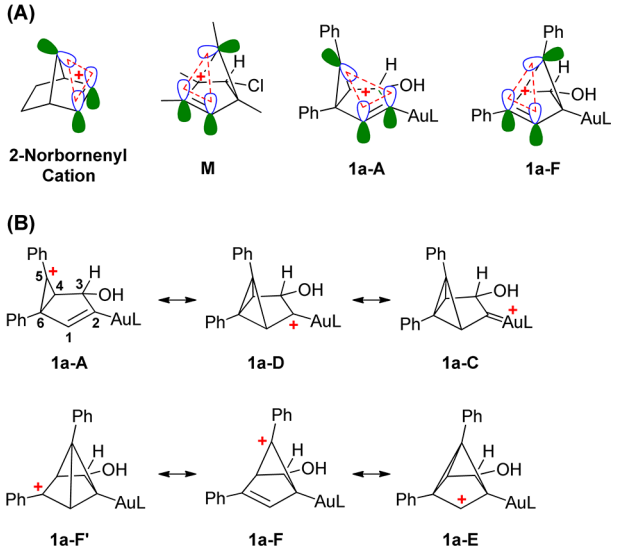

that there are only weak interactions between the cationic center C5 and the double bond. This may result from that the Au-linked carboanion C2 is bonded with C5 and thus stabilizes the carbocation. As shown in Scheme 6B, the resonance structures indicate that **A**, **D**, and **C** shown in Scheme 2 are actually one species, and so are **F** and **E**. The atoms in molecules (AIM)[12,18d,e,21] topological analysis on intermediates **A** and **F** for substrates **1a**, **1b**, and **1c′** (using methyl groups instead of *n*Bu groups in **1c**) has been done (Figure 3). The results show that for **1c′-A** and **1c′-F**, there do exist bond path and bond critical points between C5 and C1, which are similar to a 1,2,4,7-antitetramethyl-2-norbornyl cation with a C−C bond distance of 1.710 Å.[12a] The larger Wiberg bond indices (WBI)[21d] of C1−C5 in **1c′-A** and **1c′-F** also indicate stronger interaction.

Nature of the 1,3-Cationic Alkylidene Migration. To disclose the nature of this 1,3-cationic alkylidene migration, the 1,3-alkyl migration of neutral molecule 5-*exo*-methylbicyclo [2.1.1] hex-2-ene (**K**) to 6-*exo*-methylbicyclo [3.1.0] hex-2-ene (**L**) was used as a reference system (Scheme 7A).[9a−c] The framework rearrangement of **K** to **L** is similar to that of **1a-F** to **1a-A** or **1a-J**, both involving isomerization between [2.1.1] and [3.1.0] bicyclic structures. Theoretical studies[22] show that the isomerization of **K** to **L** may involve a diradical mechanism, and the reaction barrier is higher than 30 kcal/mol, which is consistent with the high reaction temperature of 120 °C. In the transition state **TS-KL**, the bridging carbon C5 is far away from both C2 and C6 (2.470 and 2.424 Å, respectively);[22b] that is, the old bond is broken, but the new one is not formed yet. This may account for the high reaction barrier.

The isomerization of **1a-A** to **1a-F** and **1a-F** to **1a-J** is very easy, and the barriers are only 1.5 and 12.3 kcal/mol, respectively. However, the barrier of the isomerization of **L** to **K** is higher than 54.1 kcal/mol. In transition state **1a-3-TS1**, the C5−C6 bond is not fully broken (1.476 Å), and C5 has strong interaction with C1 (1.658 Å) and C2 (2.176 Å). In transition state **1a-3-TS2**, the C5−C4 bond is nearly broken

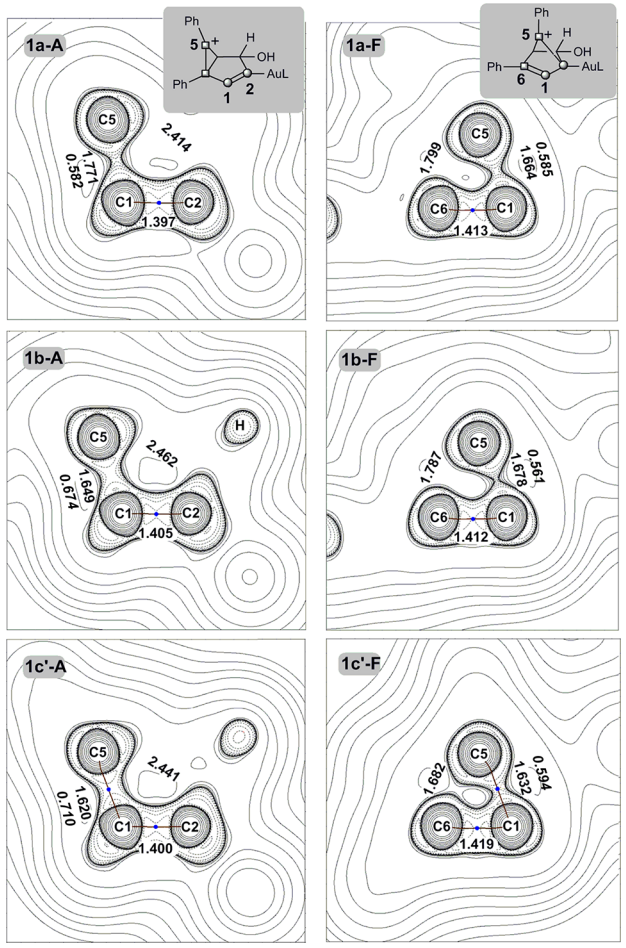

Figure 3. The molecule graphs and the Laplacian of the electron density distribution ($\nabla^2\rho$) of the positive C5 and the double bond C1−C2/C6−C1 plane in intermediates **A** and **F** for substrates **1a**, **1b**, and **1c′** ($R^2 = R^3$ = Me). The blue points indicate the bond critical points, and the black lines between the atom pair are bond paths. The selected bond lengths are in antstroms. The Wiberg bond indices (WBI) of C1−C5 are given in italic.

(2.068 Å), but the C5−C1 bond is nearly fully formed (1.489 Å). A depiction of the orbital interactions in 1,3-cationic alkylidene migration between **1a-A** and **1a-F** is proposed in Scheme 7B based on an inspection of the MOs of these species.[8] For **1a-A**, one p orbital and one sp^2 orbital on C5 are involved in the 1,3-cationic alkylidene migration: the p orbital containing the positive charge attacks the double bond, overlaps with the p orbital on C2, and evolves into a sp^2 orbital, forms the new C5−C2 σ bond; the C5−C6 σ bond breaks, the sp^2 orbital on C5 evolves into the p orbital containing the positive charge, and the sp^2 orbital on C6 evolves into the p orbital of the new double bond. Thus, the easy 1,3-cationic alkylidene migration of **A** to **F** and **F** to **J** may be ascribed to the strong interaction between the carbocation C5 and the double bond on the five-membered ring. To test this hypothesis, the isomerization of $\mathbf{L}^+$, which is formed by abstracting a hydride from C5 in **L**, was calculated. As expected, the isomerization barrier of $\mathbf{L}^+$ to $\mathbf{K}^+$ is only 1.6 kcal/mol, which is similar to that of **1a-A** to **1a-F**. Therefore, this easy 1,3-migration is promoted by the strong cation−π interaction in the nonclassical carbocations.

dx.doi.org/10.1021/ja410734e | J. Am. Chem. Soc. 2014, 136, 1505−1513

Scheme 7. (A) Depiction of Orbital Interactions in the 1,3-Alkyl Migration of K to L Based on Ref 22b; (B) Depiction of Orbital Interactions in the 1,3-Cationic Alkylidene Migration of the Nonclassical Carbocation 1a-A to 1a-F; and (C) 1,3-Cationic Alkylidene Migration of L^+ to K^+[a]

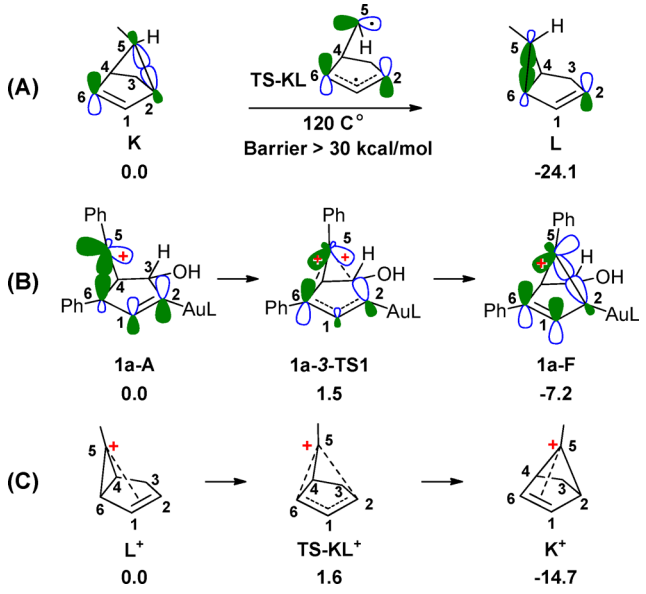

[a]The data in (B) and (C) were calculated at the PBE1PBE/6-31+G**/SDD level; the relative free energies in solvent ΔG_{sol} (298.15 K, 1.0 atm) are in kcal/mol. Here, **K**, **1a-A**, and L^+ are used as the zero energy reference points, respectively.

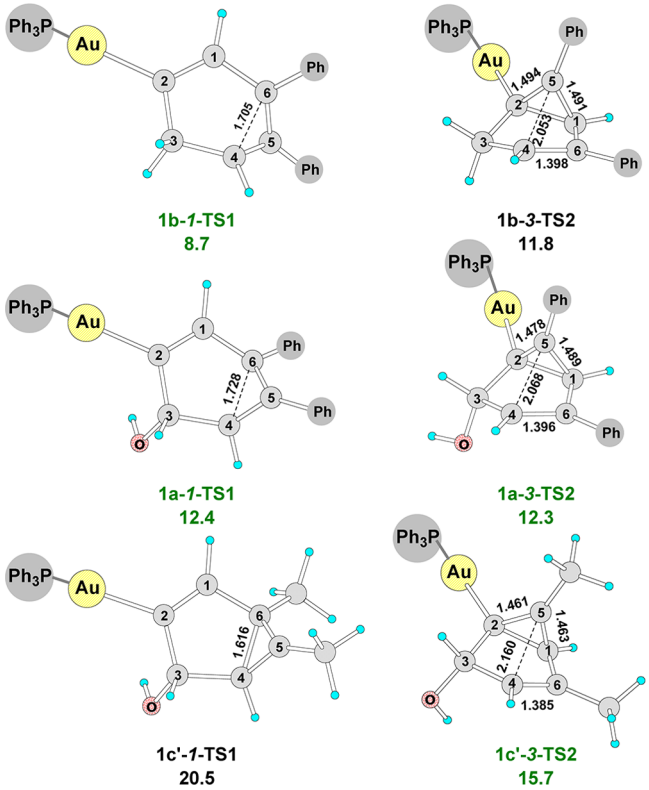

Figure 4. The transition states of the rate-determining steps along ***Path-1*** and ***Path-3*** of substrates **1a**, **1b**, and **1c′**. Here, **1a-F**, **1b-F**, and **1c′-F** were used as the zero energy reference points, respectively. The details of the Ph groups and the PPh_3 ligand are not shown for clarity. The selected bond lengths are in angstroms. The relative free energies in solvent ΔG_{sol} (298.15 K, 1.0 atm) are in kcal/mol. The green numbers indicate the favorable transition states. Calculated at the PBE1PBE/6-31+G**/SDD level.

In Wagner–Meerwein rearrangement, the nucleophilic alkyl group moves to an adjacent carbocation via 1,2-migration to generate another more stable carbocation species, and at the position where the alkyl group left forms the new cationic center (Scheme 2). However, in the 1,3-cationic alkylidene migration here, it is the cationic center C5 that migrates, and the cationic center remains on C5 in the whole process. The 1,4-carbon migration of cation obtained by removing the hydride on C3 in **L** has been studied by Winstein et al.[9d–f] In this structure, the positive charges delocalize on the five-membered ring. Recently, we also found 1,3-cationic alkylidene migration in 1,6-enyne cycloisomerization reactions.[23] Therefore, this reaction pattern might be expected to have some broader applications.

Origin of the Product Selectivity of 2 and 3. As shown in Scheme 4, the rate-determining steps of ***Path-1*** and ***Path-3*** are the ring-enlargement process (**1a-1-TS1**) and the second 1,3-cationic alkylidene migration process (**1a-3-TS2**), respectively. As compared to these two rate-determining steps, the barrier of the first 1,3-cationic alkylidene migration (**1a-3-TS1**) is much lower and therefore very fast, and so the intermediate **1a-A** should transform to **1a-F** quickly. Therefore, **1a-F** is the "real reactant" for the competing reactions along ***Path-1*** and ***Path-3***. For convenience, in this section, **1a-F**, **1b-F**, and **1c′-F** were used as the zero energy reference points, respectively. The calculated results of transition states **1-TS1** and **3-TS2** of substrates **1a**, **1b**, and **1c′** (Figure 4) are well consistent with the experimental observations (see Scheme 1). **1a-1-TS1** and **1a-3-TS2** have nearly identical relative energies, indicating that both **2a** and **3a** can be equally obtained (**2a**:**3a** = 1:1). For substrate **1b**, **1b-3-TS2** is 3.1 kcal/mol higher in energy than **1b-1-TS1**, indicating that only **2b** can be obtained (**2b**:**3b** = 1:0), whereas for substrate **1c′**, **1c′-3-TS2** is 4.8 kcal/mol lower in energy than **1c′-1-TS1**, which means only **3c′** can be obtained (**2c**:**3c** = 0:1), and thus the product selectivity is reversed. We found that the product selectivity can be rationalized by the electronic effects of the substituents. In the transition states, the hydroxyl groups are attached to sp^3-hybridized carbon atom C3. Therefore, only the electron-withdrawing inductive effect is working. The phenyl group has a much stronger electron-donating conjugation effect than do the alkyl groups.

In the direct ring-enlargement step (**1-TS1**), the positive charges on C5 will delocalize into the forming six-membered ring. Therefore, electron-donating groups on the six-membered ring will facilitate this process. As compared to **1a-1-TS1**, the absence of the electron-withdrawing hydroxyl group in **1b-1-TS1** accelerates the ring-enlargement. However, in **1c′-1-TS1**, the displacement of two phenyl groups with methyl groups makes the ring-enlargement much more difficult.

The 1,3-cationic alkylidene migration transition states (**3-TS2**) all partially possess nonclassical carbocation properties. In these structures, the electron density on the C=C double bond determines the ability to stabilize carbocation C5. The electron-withdrawing hydroxyl group will decrease the stabilizing effect to some degree; thus **1a-3-TS2** is higher in energy than **1b-3-TS2**. In **1c′-3-TS2**, the two phenyl groups are changed to methyl groups, and the barrier rises as expected. The charge donation from the double bond to the cationic center C5 is

dx.doi.org/10.1021/ja410734e | J. Am. Chem. Soc. 2014, 136, 1505–1513

evidenced by the C4−C6 bond elongation; that is, the longer is the bond, the lower is the energy. In **1b-3-TS2**, **1a-3-TS2**, and **1c′-3-TS2**, the C4−C6 bond lengths are 1.398, 1.396, and 1.385 Å, respectively. Possibly due to that the cationic center C5 is stabilized by the partially bonded carboanion C2, **3-TS2** is less sensitive to the electronic effects of the substituents. This leads to the reversal of the product selectivity, although the energy change of **1-TS1** and **3-TS2** has the same trend.

Unsymmetrical Substrate 1d. For the unsymmetrical substrate **1d**, only the TMS group migrated product **3d** was obtained (see Scheme 1B).[7] Therefore, **1d** is a good case to further test with the mechanism proposed in Scheme 4. The key intermediate and transition states were calculated using model **1d′** in which R^2 = Me. As shown in Scheme 8, the ring-

Scheme 8. Calculated Key Intermediate and Transition States for Substrate 1d Using 1d′ (R^2 = Me)[a]

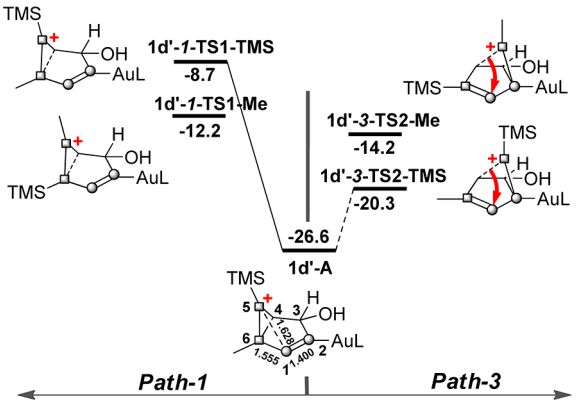

[a]The relative free energies in solvent ΔG_{sol} (298.15 K, 1.0 atm) are in kcal/mol. Calculated at the PBE1PBE/6-31+G**/SDD level. **1d′-R** is used as the zero energy reference point.[8]

enlargement processes are much higher in energy than the 1,3-migrations. The 1,3-migration of the TMS-substituted cationic alkylidene (**1d′-3-TS2-TMS**) is 6.1 kcal/mol more favorable than that of 1,3-migration of the methyl group-substituted cationic alkylidene (**1d′-3-TS2-Me**). These results are well consistent with the experimental observations and can be rationalized by strong hyperconjugation of the C8−Si bond of the TMS group to the cationic center C5. As shown in Figure 5, in **1d′-3-TS2-TMS**, the C9−Si−C5 bond angle is 109.8°. However, the C8−Si−C5 bond angle decreases to 102.9°, and the C8−Si bond obviously bends to C5, whereas in **1d′-3-TS2-Me** the smallest bond angle H−C7−C6 is 106.1°. The Si−C5 bond in **1d′-3-TS2-TMS** is shorter than that in **1d′-3-TS2-Me** (1.903 vs 1.922 Å), indicating stronger interaction between C5 and the TMS group in **1d′-3-TS2-TMS**.

CONCLUSION

DFT studies have been performed on the mechanism of gold(I)-catalyzed cycloisomerization of 1,5-enynes containing cyclopropene moiety at the PBE1PBE/6-31+G**/SDD level. An unprecedented pathway containing two consecutive 1,3-cationic alkylidene migrations of nonclassical carbocation intermediates was proposed. This 1,3-cationic alkylidene migration is promoted by strong cation−π interaction between the cationic center and the double bond. Topological analysis shows that for certain nonclassical carbocation intermediates, there do exist bond critical point and bond path between the

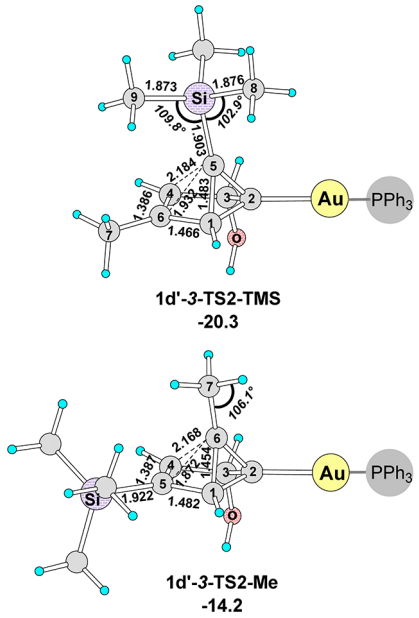

Figure 5. Structures of **1d′-3-TS2-TMS** and **1d′-3-TS2-Me** with selected bond lengths (in Å) and bond angles (in degrees). The relative free energies in solvent ΔG_{sol} (298.15 K, 1.0 atm) are in kcal/mol. Calculated at the PBE1PBE/6-31+G**/SDD level.

cationic center and the double bond. These results show that in a common reaction, typical nonclassical carbocation may be involved in and have significant effects on the reaction mechanisms. The selectivity of the initial cyclization is controlled by ring strain, and the product distribution is mainly controlled by the electronic effects of the substituents.

ASSOCIATED CONTENT

Supporting Information

Computational details, the relaxed potential energy surface (PES) scan, selected IRC calculations, selected molecular orbitals, and the calculated total energies and geometrical coordinates. This material is available free of charge via the Internet at http://pubs.acs.org.

AUTHOR INFORMATION

Corresponding Author

liyuxue@sioc.ac.cn

Notes

The authors declare no competing financial interest.

ACKNOWLEDGMENTS

This project is supported by the National Basic Research Program of China (973 Program, no. 2009CB825300) and the Natural Science Foundation of China (Grant nos. 21172248, 21372249, 21121062).

REFERENCES

(1) (a) Jiménez-Núñez, E.; Echavarren, A. M. *Chem. Commun.* **2007**, 333. (b) Fürstner, A.; Davies, P. W. *Angew. Chem., Int. Ed.* **2007**, *46*, 3410. (c) Hashmi, A. S. K. *Chem. Rev.* **2007**, *107*, 3180. (d) Gorin, D. J.; Toste, F. D. *Nature* **2007**, *446*, 395. (e) Li, Z.; Brouwer, C.; He, C. *Chem. Rev.* **2008**, *108*, 3239. (f) Arcadi, A. *Chem. Rev.* **2008**, *108*, 3266. (g) Gorin, D. J.; Sherry, B. D.; Toste, F. D. *Chem. Rev.* **2008**, *108*, 3351. (h) Sengupta, S.; Shi, X. *ChemCatChem* **2010**, *2*, 609. (i) Hashmi, A. S. K. *Angew. Chem., Int. Ed.* **2010**, *49*, 5232. (j) Miege, F.; Meyer, C.; Cossy, J. *Beilstein J. Org. Chem.* **2011**, *7*,

717. For DFT calculations related to gold catalysis, see: (k) Soriano, E.; Marco-Contelles, J. *Computational Mechanisms of Au and Pt Catalyzed Reactions*; Springer Verlag: New York, 2011; Vol. *302*. (l) Pyykkö, P. *Angew. Chem., Int. Ed.* **2004**, *43*, 4412. (m) Soriano, E.; Marco-Contelles, J. *Acc. Chem. Res.* **2009**, *42*, 1026.

(2) For gold-catalyzed cycloisomerizations of enynes, see: (a) Ma, S.; Yu, S.; Gu, Z. *Angew. Chem., Int. Ed.* **2006**, *45*, 200. (b) Michelet, V.; Toullec, P. Y.; Genêt, J.-P. *Angew. Chem., Int. Ed.* **2008**, *47*, 4268. (c) Jiménez-Núñez, E.; Echavarren, A. M. *Chem. Rev.* **2008**, *108*, 3326. (d) Patil, N. T.; Yamamoto, Y. *Chem. Rev.* **2008**, *108*, 3395. (e) Belmont, P.; Parker, E. *Eur. J. Org. Chem.* **2009**, 6075. (f) Couty, S.; Meyer, C.; Cossy, J. *Tetrahedron* **2009**, *65*, 1809.

(3) For gold-catalyzed cycloisomerizations of 1,5-enynes, see: (a) Zhang, L.; Kozmin, S. A. *J. Am. Chem. Soc.* **2004**, *126*, 11806. (b) Sun, J.; Conley, M. P.; Zhang, L.; Kozmin, S. A. *J. Am. Chem. Soc.* **2006**, *128*, 9705. (c) Nevado, C.; Echavarren, A. M. *Chem.—Eur. J.* **2005**, *11*, 3155. (d) López-Carrillo, V.; Huguet, N.; Mosquera, A.; Echavarren, A. M. *Chem.—Eur. J.* **2011**, *17*, 10972.

(4) For DFT calculations on gold-catalyzed cycloisomerizations of 1,5-enynes, see: (a) Liu, Y.; Zhang, D.; Zhou, J.; Liu, C. *J. Phys. Chem. A* **2010**, *114*, 6164. (b) Liu, Y.; Zhang, D.; Bi, S. *J. Phys. Chem. A* **2010**, *114*, 12893. (c) Fan, T.; Chen, X.; Sun, J.; Lin, Z. *Organometallics* **2012**, *31*, 4221. (d) Soriano, E.; Marco-Contelles, J. *J. Org. Chem.* **2012**, *77*, 6231. (e) Ariafard, A.; Asadollah, E.; Ostadebrahim, M.; Rajabi, N. A.; Yates, B. F. *J. Am. Chem. Soc.* **2012**, *134*, 16882.

(5) For gold-catalyzed cycloisomerizations of 1,6-enynes, see: (a) Nieto-Oberhuber, C.; Muñoz, M. P.; Buñuel, E.; Nevado, C.; Cárdenas, D. J.; Echavarren, A. M. *Angew. Chem., Int. Ed.* **2004**, *43*, 2402. (b) Nieto-Oberhuber, C.; López, S.; Muñoz, M. P.; Cárdenas, D. J.; Buñuel, E.; Nevado, C.; Echavarren, A. M. *Angew. Chem., Int. Ed.* **2005**, *44*, 6146. (c) Bruneau, C. *Angew. Chem., Int. Ed.* **2005**, *44*, 2328. (d) Nieto-Oberhuber, C.; López, S.; Jiménez-Núñez, E.; Echavarren, A. M. *Chem.—Eur. J.* **2006**, *12*, 5916. (e) Nieto-Oberhuber, C.; Pérez-Galán, P.; Herrero-Gómez, E.; Lauterbach, T.; Rodríguez, C.; López, S.; Bour, C.; Rosellón, A.; Cárdenas, D. J.; Echavarren, A. M. *J. Am. Chem. Soc.* **2008**, *130*, 269. For DFT calculations on gold-catalyzed cycloisomerizations of 1,6-enynes, see: (f) Zhuo, L. G.; Zhang, J. J.; Yu, Z. X. *J. Org. Chem.* **2012**, *77*, 8527. (g) Muuronen, M.; Perea-Buceta, J. E.; Nieger, M.; Patzschke, M.; Helaja, J. *Organometallics* **2012**, *31*, 4320.

(6) (a) Meerwein, H.; van Emster, K. *Chem. Ber.* **1922**, *55*, 2500. (b) Birladeanu, L. *J. Chem. Educ.* **2000**, *77*, 858. (c) Ghorpade, S.; Su, M.-D.; Liu, R.-S. *Angew. Chem., Int. Ed.* **2013**, *52*, 4229.

(7) Li, C.; Zeng, Y.; Zhang, H.; Feng, J.; Zhang, Y.; Wang, J. *Angew. Chem., Int. Ed.* **2010**, *49*, 6413.

(8) See the Supporting Information for more details.

(9) For 1,3-carbon migration via diradical mechanism, see: (a) Roth, W. R.; Friedrich, A. *Tetrahedron Lett.* **1969**, *10*, 2607. (b) Leber, P. A.; Baldwin, J. E. *Acc. Chem. Res.* **2002**, *35*, 279. (c) Baldwin, J. E.; Leber, P. A. *Org. Biomol. Chem.* **2008**, *6*, 36. For 1,4-carbon migration, see: (d) Childs, R. F.; Winstein, S. *J. Am. Chem. Soc.* **1968**, *90*, 7146. (e) Childs, R. F.; Winstein, S. *J. Am. Chem. Soc.* **1974**, *96*, 6409. (f) Genaev, A. M.; Sal'nikov, G. E.; Shubin, V. G. *Russ. J. Org. Chem.* **2007**, *43*, 1134. For literature mentioning nonlcassical carbocation in mechanism study, see: (g) Madhushaw, R. J.; Lo, C.-Y.; Hwang, C.-W.; Su, M.-D.; Shen, H.-C.; Pal, S.; Shaikh, I. R.; Liu, R.-S. *J. Am. Chem. Soc.* **2004**, *126*, 15560. (h) Lin, M.-Y.; Das, A.; Liu, R.-S. *J. Am. Chem. Soc.* **2006**, *128*, 9340. (i) Tang, J.-M.; Bhunia, S.; Sohel, S. M. A.; Lin, M.-Y.; Liao, H.-Y.; Datta, S.; Das, A.; Liu, R.-S. *J. Am. Chem. Soc.* **2007**, *129*, 15677. (j) Garayalde, D.; Gómez-Bengoa, E.; Huang, X.; Goeke, A.; Nevado, C. *J. Am. Chem. Soc.* **2010**, *132*, 4720.

(10) (a) Winstein, S.; Trifan, D. S. *J. Am. Chem. Soc.* **1949**, *71*, 2953. (b) Winstein, S.; Trifan, D. *J. Am. Chem. Soc.* **1952**, *74*, 1147. (c) Winstein, S.; Trifan, D. *J. Am. Chem. Soc.* **1952**, *74*, 1154. (d) Winstein, S.; Shatavsky, M.; Norton, C.; Woodward, R. B. *J. Am. Chem. Soc.* **1955**, *77*, 4183. (e) Winstein, S.; Clippinger, E.; Howe, R.; Vogelfanger, E. *J. Am. Chem. Soc.* **1965**, *87*, 376. (f) Brookhar, M.; Diaz, A.; Winstein, S. *J. Am. Chem. Soc.* **1966**, *88*, 3135. (g) Richey, H. G.; Nichols, J. D.; Gassman, P. G.; Fentiman, A. F.; Winstein, S.; Brookhar, M.; Lustgart, R. K. *J. Am. Chem. Soc.* **1970**, *92*, 3783. (h) Schulman, J. M.; Disch, R. L.; Schleyer, P. V.; Buhl, M.; Bremer, M.; Koch, W. *J. Am. Chem. Soc.* **1992**, *114*, 7897. (i) Olah, G. A.; Prakash, G. K. S.; Saunders, M. *Acc. Chem. Res.* **1983**, *16*, 440. (j) Laube, T.; Lohse, C. *J. Am. Chem. Soc.* **1989**, *111*, 9224. (k) Laube, T.; Lohse, C. *J. Am. Chem. Soc.* **1994**, *116*, 9001. (l) Laube, T. *Acc. Chem. Res.* **1995**, *28*, 399. (m) Olah, G. A. *Angew. Chem., Int. Ed.* **1995**, *34*, 1393. (n) Laube, T. *J. Am. Chem. Soc.* **2004**, *126*, 10904. (o) Scholz, F.; Himmet, D.; Heinemann, F. W.; Schleyer, P. v. R.; Meyer, K.; Krossing, I. *Science* **2013**, *341*, 62.

(11) Theoretical studies on nonclassical carbocation: (a) Schleyer, P. v. R.; Maerker, C. *Pure Appl. Chem.* **1995**, *67*, 755. (b) Tantillo, D. J.; Hietbrink, B. N.; Merlic, C. A.; Houk, K. N. *J. Am. Chem. Soc.* **2000**, *122*, 7136. (c) Olah, G. A.; Rasul, G.; Surya Prakash, G. K. *J. Org. Chem.* **2000**, *65*, 5956. (d) Smith, W. B. *J. Org. Chem.* **2001**, *66*, 376. (e) Eckert-Maksić, M.; Antol, I.; Margetić, D.; Glasovac, Z. *J. Chem. Soc., Perkin Trans. 2* **2002**, 2057. (f) Alkorta, I.; Abboud, J. L. M.; Quintanilla, E.; Dávalos, J. Z. *J. Phys. Org. Chem.* **2003**, *16*, 546. (g) Antol, I.; Glasovac, Z.; Eckert-Maksić, M. *New J. Chem.* **2004**, *28*, 880. (h) Reddy, V. P.; Rasul, G.; Prakash, G. K. S.; Olah, G. A. *J. Org. Chem.* **2007**, *72*, 3076. (i) Hong, Y. J.; Tantillo, D. J. *J. Org. Chem.* **2007**, *72*, 8877. (j) Hong, Y. J.; Tantillo, D. J. *Chem. Sci.* **2013**, *4*, 2512. (k) Tantillo, D. J.; Schleyer, P. v. R. *Org. Lett.* **2013**, *15*, 1725. (l) Gutierrez, O.; Harrison, J. G.; Felix, R. J.; Cortés Guzman, F.; Gagné, M. R.; Tantillo, D. J. *Chem. Sci.* **2013**, *4*, 3894.

(12) Literature on AIM topological analysis on nonclassical carbocation: (a) Muchall, H. M.; Werstiuk, N. H. *J. Phys. Chem. A* **1999**, *103*, 6599. (b) Werstiuk, N. H.; Muchall, H. M. *J. Phys. Chem. A* **2000**, *104*, 2054. (c) Werstiuk, N. H.; Muchall, H. M.; Noury, S. *J. Phys. Chem. A* **2000**, *104*, 11601. (d) Werstiuk, N. H. *J. Chem. Theory Comput.* **2007**, *3*, 2258. (e) Firme, C. L.; Antunes, O. A. C.; Esteves, P. M. *J. Phys. Chem. A* **2008**, *112*, 3165. (f) Firme, C. L.; Antunes, O. A. C.; Esteves, P. M. *J. Braz. Chem. Soc.* **2009**, *20*, 543. (g) Werstiuk, N. H.; Poulsen, D. A. *ARKIVOC* **2009**, 38. (h) Rzepa, H. S.; Allan, C. S. M. *J. Chem. Educ.* **2010**, *87*, 221.

(13) (a) Hohenberg, P.; Kohn, W. *Phys. Rev.* **1964**, *136*, B864. (b) Kohn, W.; Sham, L. J. *Phys. Rev.* **1965**, *140*, A1133.

(14) (a) Perdew, J. P.; Burke, K.; Ernzerhof, M. *Phys. Rev. Lett.* **1996**, *77*, 3865. (b) Perdew, J. P.; Burke, K.; Ernzerhof, M. *Phys. Rev. Lett.* **1997**, *78*, 1396. (c) Adamo, C.; Barone, V. *J. Chem. Phys.* **1999**, *110*, 6158.

(15) Frisch, M. J.; Trucks, G. W.; Schlegel, H. B.; Scuseria, G. E.; Robb, M. A.; Cheeseman, J. R.; Scalmani, G.; Barone, V.; Mennucci, B.; Petersson, G. A.; Nakatsuji, H.; Caricato, M.; Li, X.; Hratchian, H. P.; Izmaylov, A. F.; Bloino, J.; Zheng, G.; Sonnenberg, J. L.; Hada, M.; Ehara, M.; Toyota, K.; Fukuda, R.; Hasegawa, J.; Ishida, M.; Nakajima, T.; Honda, Y.; Kitao, O.; Nakai, H.; Vreven, T.; Montgomery, J. A., Jr.; Peralta, J. E.; Ogliaro, F.; Bearpark, M.; Heyd, J. J.; Brothers, E.; Kudin, K. N.; Staroverov, V. N.; Kobayashi, R.; Normand, J.; Raghavachari, K.; Rendell, A.; Burant, J. C.; Iyengar, S. S.; Tomasi, J.; Cossi, M.; Rega, N.; Millam, N. J.; Klene, M.; Knox, J. E.; Cross, J. B.; Bakken, V.; Adamo, C.; Jaramillo, J.; Gomperts, R.; Stratmann, R. E.; Yazyev, O.; Austin, A. J.; Cammi, R.; Pomelli, C.; Ochterski, J. W.; Martin, R. L.; Morokuma, K.; Zakrzewski, V. G.; Voth, G. A.; Salvador, P.; Dannenberg, J. J.; Dapprich, S.; Daniels, A. D.; Farkas, Ö.; Foresman, J. B.; Ortiz, J. V.; Cioslowski, J.; Fox, D. J. *Gaussian 09*, revision A.02; Gaussian, Inc.: Wallingford, CT, 2009.

(16) Kang, R. H.; Chen, H.; Shaik, S.; Yao, J. N. *J. Chem. Theory Comput.* **2011**, *7*, 4002.

(17) Fuentealba, P.; Preuss, H.; Stoll, H.; Von Szentpály, L. *Chem. Phys. Lett.* **1982**, *89*, 418.

(18) (a) Hirshfeld, F. L. *Theor. Chem. Acc.* **1977**, *44*, 129. (b) Ritchie, J. P. *J. Am. Chem. Soc.* **1985**, *107*, 1829. (c) Ritchie, J. P.; Bachrach, S. M. *J. Comput. Chem.* **1987**, *8*, 499. (d) Lu, T.; Chen, F. *J. Comput. Chem.* **2012**, *33*, 580. (e) Lu, T.; Chen, F. *J. Mol. Graphics Modell.* **2012**, *38*, 314.

(19) (a) Cancès, E.; Mennucci, B.; Tomasi, J. *J. Chem. Phys.* **1997**, *107*, 3032. (b) Mennucci, B.; Tomasi, J. *J. Chem. Phys.* **1997**, *106*, 5151.

(20) Frisch, M. J.; Trucks, G. W.; Schlegel, H. B.; Scuseria, G. E.; Robb, M. A.; Cheeseman, J. R.; Montgomery, J. A., Jr.; Vreven, T.; Kudin, K. N.; Burant, J. C.; Millam, J. M.; Iyengar, S. S.; Tomasi, J.; Barone, V.; Mennucci, B.; Cossi, M.; Scalmani, G.; Rega, N.; Petersson, G. A.; Nakatsuji, H.; Hada, M.; Ehara, M.; Toyota, K.; Fukuda, R.; Hasegawa, J.; Ishida, M.; Nakajima, T.; Honda, Y.; Kitao, O.; Nakai, H.; Klene, M.; Li, X.; Knox, J. E.; Hratchian, H. P.; Cross, J. B.; Bakken, V.; Adamo, C.; Jaramillo, J.; Gomperts, R.; Stratmann, R. E.; Yazyev, O.; Austin, A. J.; Cammi, R.; Pomelli, C.; Ochterski, J. W.; Ayala, P. Y.; Morokuma, K.; Voth, G. A.; Salvador, P.; Dannenberg, J. J.; Zakrzewski, V. G.; Dapprich, S.; Daniels, A. D.; Strain, M. C.; Farkas, Ö.; Malick, D. K.; Rabuck, A. D.; Raghavachari, K.; Foresman, J. B.; Ortiz, J. V.; Cui, Q.; Baboul, A. G.; Clifford, S.; Cioslowski, J.; Stefanov, B. B.; Liu, G.; Liashenko, A.; Piskorz, P.; Komaromi, I.; Martin, R. L.; Fox, D. J.; Keith, T.; Al-Laham, M. A.; Peng, C. Y.; Nanayakkara, A.; Challacombe, M.; Gill, P. M. W.; Johnson, B.; Chen, W.; Wong, M. W.; Gonzalez, C.; Pople, J. A. *Gaussian 03*, revision C.02; Gaussian, Inc.: Wallingford, CT, 2004.

(21) (a) Bader, R. F. W. *Acc. Chem. Res.* **1985**, *18*, 9. (b) Bader, R. F. W. *Atoms in Molecules: A Quantum Theory*; Clarendon Press: Oxford, 1990. (c) Bader, R. F. W. *Chem. Rev.* **1991**, *91*, 893. (d) Wiberg, K. B. *Tetrahedron* **1968**, *24*, 1083.

(22) (a) Suhrada, C. P.; Houk, K. N. *J. Am. Chem. Soc.* **2002**, *124*, 8796. (b) Tao, H.-R.; Fang, D.-C. *Theor. Chem. Acc.* **2008**, *121*, 91. (c) Williams, A. *Concerted Organic and Bio-Organic Mechanisms*; CRC Press: New York, 2000. (d) Dewar, M. J. S. *J. Am. Chem. Soc.* **1984**, *106*, 209. (e) Hess, B. A.; Smentek, L. *Org. Biomol. Chem.* **2012**, *10*, 7503. (f) Tantillo, D. J. *J. Phys. Org. Chem.* **2008**, *21*, 561.

(23) This work is being undertaken in our group.